GaAsSbN for Multi-Junction Solar Cells

A. Mumtaz, M. Milanova, I. Sandall, K. Cheetham, Z. Cao, M. Bilton, G. Piana, N. Fleck, L. Phillips, O. Hutter, V. Donchev, K. Durose,

***Abstract*—Multi-junction solar cells, according to the detailed balance limit, should be able to achieve efficiencies above 50 percent. Work on new materials is necessary for improvements beyond the current state of the art. In this work, we evaluate the use of GaAsSbN, which has shown promise for multi-junction solar cells, particularly targeting the 1eV cell. Epitaxial growth of this material in this work has been achieved via liquid phase epitaxy, as it can produce high quality crystalline layers. We present our initial growth and characterization results of a GaAsSbN layer. Also presented are results showing the incorporation of this material in a solar cell.**

Keywords—GaAsSbN, III-V, liquid phase epitaxy, multijunction solar cells

I. Introduction

The highest efficiency solar cells are currently based on multi junctions, targeting complimentary regions of the solar spectrum. The highest efficiency three junction solar cell developed by Sharp, is an inverted metamorphic design achieving an efficiency of 44.4% under a concentration of 302 suns. This solar cell was based on an InGaP top layer, GaAs middle layer and an InGaAs bottom layer, fabricated on a silicon wafer. For four junction solar cells the highest efficiency attained is 46% and was for a concentrator solar cell based on GaInP (1.9eV), GaAs (1.4eV), GaInAsP (1.1eV) and GaInAs (0.7eV) [1]. This was achieved at a concentration of 508 suns. A wafer bonding step was used in its fabrication. NREL has recently produced a 6-junction cell with an efficiency of 47.1%.

Calculations based on the detailed balance limit have proposed a maximum theoretical efficiency of ~68% based on maximum concentration for four junction solar cells [2][3], assuming ideal materials. A number of papers have proposed efficiencies over 50% using alternate multi-junction solar cell structures. One of the earlier proposals for such a four-junction cell, was using GaInP, GaAs, a third layer and Ge, with the third layer having a target bandgap of around 1eV [4]. One very early candidate for this 1eV band gap material was GaInNAs, which can also be lattice matched to GaAs. GaInNAs is a dilute nitride and the concentration of nitrogen controls the bandgap, which is explained by the band anti crossing model [5]. Despite having the ideal band gap, the resulting solar cell's current and voltage were lower than expected, which was due to the low minority carrier diffusion length of the material [6][7]. As a consequence, this drove research towards alternatives, including the GaInAs [8], producing promising efficiencies despite the need for a metamorphic buffer layer. From a manufacturing perspective to have epitaxial growth to either GaAs or Ge is preferred, avoiding the need for buffer layers. Hence there has been exploration of different materials targeting the 1eV layer, including, III-V-bismides [9] and GaAsSbN alloys [10][11].

GaAsSbN has the advantage of being a dilute nitride and its band gap can be controlled effectively through adjusting the proportion of antimony (Sb) and nitrogen (N) to GaAs. Also, variations in the Sb content affects the valence band offset while the nitrogen content primarily affects the conduction band offset. This makes it possible to tune the conduction and valence band offsets independently, while keeping the lattice matching to GaAs or Ge. This quaternary compound GaAsSbN has not been studied as extensively as GaInNAs. GaAsSbN has an advantage over GaInNAs in that the nitrogen related defects observed in the latter, are reduced in the former, due to the absence of Sn and the presence of Sb [12]. Also, the incorporation of Sb can improve crystal quality since it acts as a surfactant to reduce island formation [13]. As a consequence, the photocurrent performance of GaAsSbN can be superior to that of GaInNAs [14].

In previous works GaAsSbN layers have been fabricated using Molecular Beam Epitaxy (MBE) or Metalorganic Vapour Phase Epitaxy (MOVPE). MOVPE growth of dilute nitrides can cause unintentional carbon contamination [15], which is correlated with low minority carrier lifetime, resulting in poor solar cell performance [16]. The contamination is a consequence of the precursor gas used. In this paper we present an alternate growth method for GaAsSbN layers using liquid phase epitaxy (LPE). LPE has been used since the 1960s, and offers advantages such as low cost, simplicity and ability to grow high quality crystal layers. The high-quality layers are as a consequence of the fact that the LPE process occurs at near thermodynamic equilibrium.

In this paper we present our initial attempts at the growth of GaAsSbN layers and also a complete single junction solar cell based on GaAsSbN.

II. EXPERIMENTAL METHODS

A variety of GaAsSbN, GaAsSb and GaAs layers were grown on a semi-insulating (1 0 0) oriented undoped GaAs substrates, using the horizontal graphite slide boat technique based LPE system. GaAs substrates were appropriately etched/cleaned prior to growth. This paper presents results for the LPE films that were initially grown at the University of Liverpool. Also presented are results of PL spectra and complete p-i-n solar cell

device fabricated at the Bulgarian Academy of Sciences Central Lab of Applied Physics. The approach used at the University of Liverpool is described below and method used for the single GaAsSbN layer and complete solar cell made at the Bulgarian Academy of Sciences Central Lab of Applied Physics is described in [17][18].

In order to obtain a more uniform structure, a low LPE growth temperature ($T_{crystallization}$ < 600°C) was chosen. Also, due to the large miscibility region for GaAsSbN and GaAsSb the compositions were carefully chosen to obtain films without phase separation. The crystallization was carried out from a melt solution comprising of 95% Ga and 5% Sb (both 6N purity). Pieces of GaAs wafer and GaN powder were used as sources of As and N, respectively. Prior to the LPE, the system was cleaned using a bake out. Then the charged graphite boat was annealed at 700°C for 2 hours under Pd-diffused ultra-pure hydrogen flow, in order to homogenize the melt and to reduce the residual impurities. Epitaxial layers were deposited from an initial temperature of 557°C. The epitaxial growth occurred from a super-cooled melt at a cooling rate of 0.8°C/minute for 10-15 minutes.

SEM and EDX analysis were carried out using a JEOL 7001 FEGSEM. TEM sections were prepared using a Helios Nanolab 600i SEM/FIB system for STEM examination in a JEOL 2000FX. Raman spectrometry was undertaken using a Renishaw inVia instrument with 1800 groves/mm grating and 532 nm laser, with spot size of 2 μm. Photoluminescence (PL) spectroscopy was also undertaken for the samples. PL spectra were measured using laser excitation at 680 nm, with power of 550 μW. The temperature dependence of the PL was recorded at single spots on the sample. The temperature range was 15300 K, with 5 K increments up to 100 K and 10 K increments up to 300 K.

For the complete solar cell, J-V and EQE measurements were performed and subsequent results are presented in this paper. The J-V measurements were completed using a TS Space Systems solar simulator with an AM1.5 spectrum at 1000 W/m^2. The EQE measurements were performed using a Bentham PVE 300 system. C-V measurements were also undertaken in this work.

III. RESULTS

A. SEM, STEM images, EDX analysis

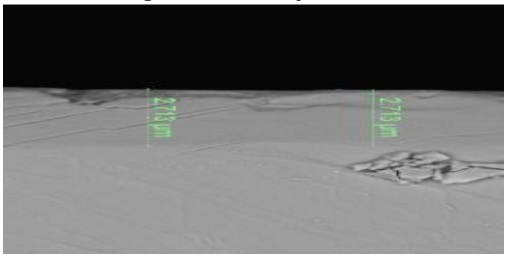

Fig. 1. SEM cross-section of a single LPE grown layer on GaAs substrate.

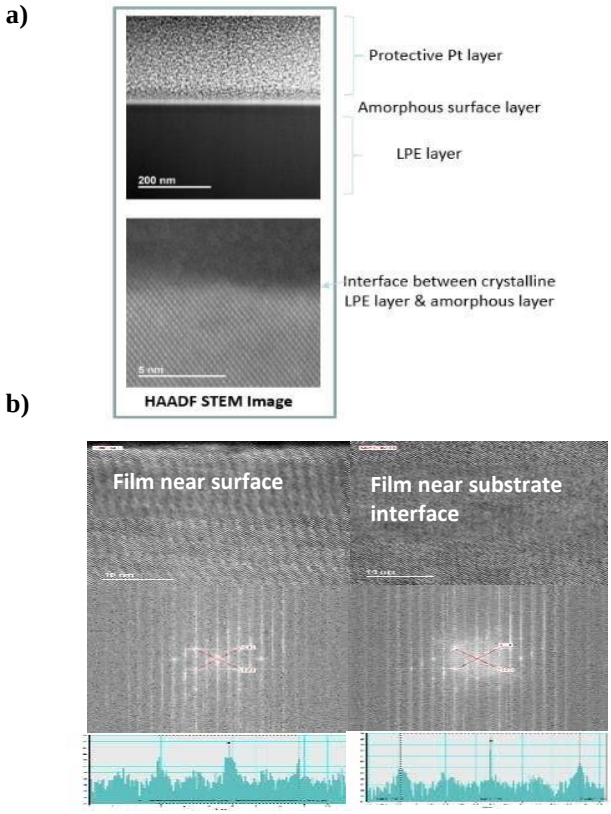

Fig. 2. a) HAADF STEM image b) STEM image, diffraction pattern and linescans at the LPE grown layer at surface and near the substrate interface.

Fig. 1 shows the SEM cross-section of a the single LPE grown layer on GaAs substrate. Indicating an approximate thickness of 2.7μm. Fig. 2 shows the TEM imaging and diffraction results

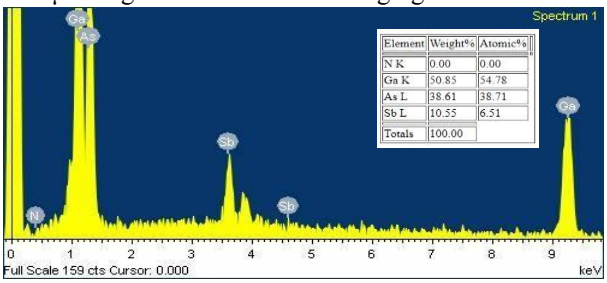

Fig. 3. Energy Dispersive X-Ray Spectroscopy of the LPE grown layer

from the LPE grown film, confirming its epitaxial crystalline character throughout the thickness of layer. The images show no evidence of phase separation. Fig. 2a is the HAADF STEM image at the top of the sample, where the Pt protective layer can also be seen, which was used to protect the surface from focused ion beam used during the sample preparation. Despite this a thin amorphous surface layer can be seen. High resolution imaging and diffraction was undertaken at the top and near the GaAs substrate to confirm the lattice parameter throughout the epitaxial layer. The STEM data analysis demonstrated that the lattice constant remains consistent throughout, from the top surface of the layer and at the substrate interface. The epitaxial layer is grown on (100) GaAs substrates, with the TEM taken through the (111) plane. The Ga, As and Sb are clearly visible in the EDX spectrum in Fig. 3. As was expected the very small

incorporation of the N appears to be below the EDX sensitivity limit.

B. Raman Spectroscopy

The LPE film was also characterized by Raman spectroscopy. Fig. 4 shows the Raman spectrum for the LPE grown layer at room temperature in comparison with the spectrum of *n*-type GaAsSbN.

The result consists of two GaAs-like sharp LO and TO lines at approximately 284 cm^{-1} and 263 cm^{-1} and they are red shifted in comparison with the phonon modes of GaAs influenced by the different material composition. The peaks in the range 150 cm^{-1} - 180 cm^{-1} can be attributed to the zone boundary LA (X) phonons. Such peaks were reported for MBE grown and annealed GaAsSbN samples [19]. Second order scattering of the GaAs peaks was observed over a frequency range 500 cm^{-1} to 550 cm^{-1}. It revealed significant reduction of the intensity of the GaAs-like LO peak and an increase in intensity of the forbidden TO peak due to the perturbation of the host lattice by the incorporation of *p*-type dopants. Both LO and TO peaks are red shifted in comparison with the phonon modes of *n*-type GaAsSbN. Subsequent Hall effect analysis on the LPE grown layers clearly demonstrated that the layers exhibited *p*-type conductivity.

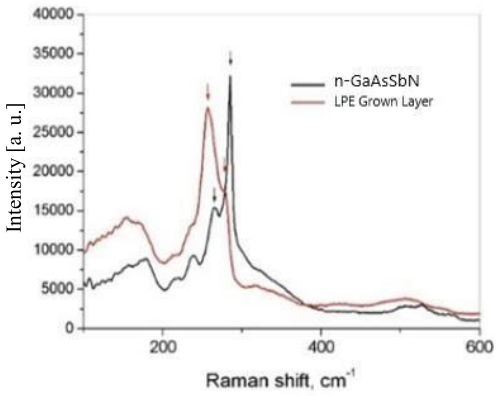

Fig. 4. Raman Spectra of LPE grown films grown on GaAs substrates.

C. Photoluminescence (PL) Spectroscopy

A comparison of the optical emission from GaAsSbN and GaAsSb layers is depicted in fig. 5. It is clear figure from that there is red shift of about 20 nm for GaAsSbN as compared to the GaAsSb layer. In addition, the optical emission of GaAsSbN layers was investigated by means of temperaturedependent PL measurements. The signal due to the GaAs substrate and the GaAsSbN epitaxial layer can clearly be seen in Fig. 6a. The bandgap of the GaAsSbN appears to be 1.29 eV and the PL signal from the GaAs substrate was attenuated by the epitaxial layer. Fig. 6b demonstrates the typical signature observed in these materials. The peak position in the PL follows a S-shape characteristic (shown as a dotted line in the figure) with increasing temperature. This is initially due to the carrier localization effects caused by compositional fluctuations. At low temperatures, the carriers are trapped in Sb or N-related localized states. As the temperature increases, the carriers gain sufficient thermal energy to escape from the localized states and hence the PL peak energy increases. At higher temperatures, it follows the expected decrease, due to the decrease in band gap.

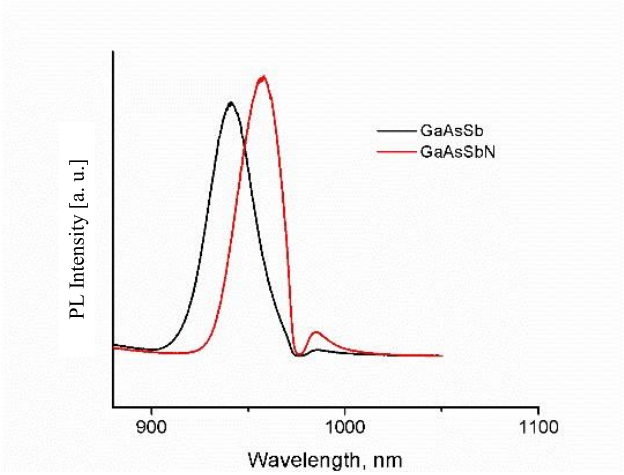

Fig. 5. A comparison of PL spectra of GaAsSbN and GaAsSb

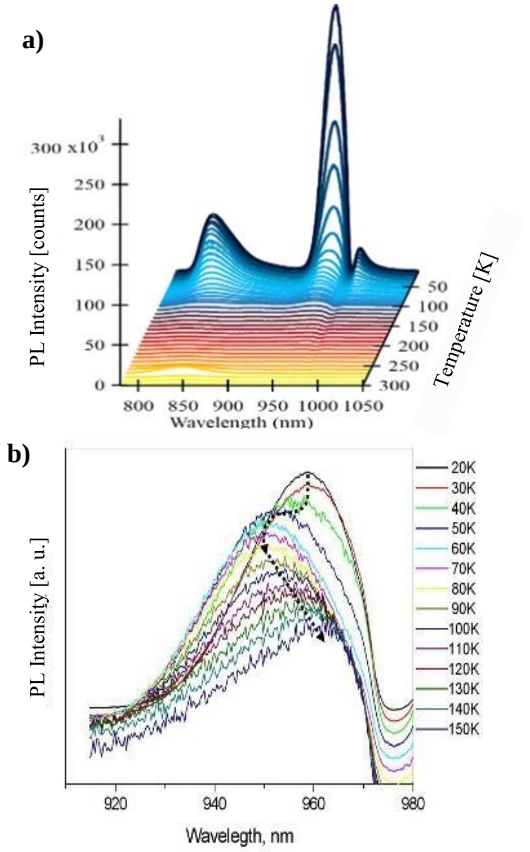

Fig. 6. a) PL spectra of GaAsSbN on GaAs substrate b) PL spectra of GaAsSbN depicting the "S" type characteristic with increasing temperature.

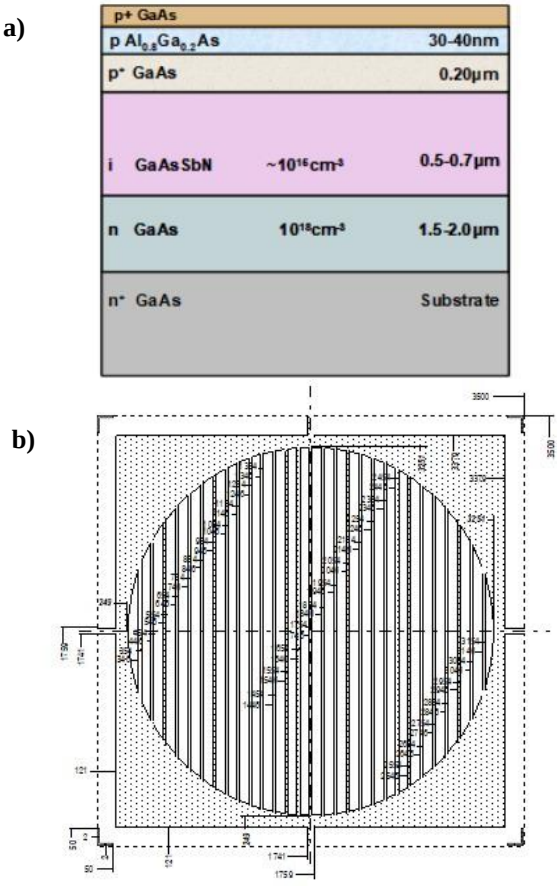

Fig. 7. a) Cross section of *p-i-n* GaAsSbN solar cell b) Top *p*-contact grid

D. Solar Cell Measurements

Once the GaAsSbN was carefully characterized, *p-i-n* based solar cells were created using LPE. A cross section of one of the solar cells can be seen in Fig. 7a. The *p-i-n* structure was employed as a consequence of the relatively low carrier diffusion length typically observed in dilute nitrides. This configuration enables improved field aided photocarrier collection. An additional top layer of highly doped p^+ GaAs was grown in order to achieve better Ohmic contacts. The AlGaAs is a window layer used to enable a reduced recombination rate at the GaAs/AlGaAs interface. The top AlGaAs and GaAs layers were also selectively etched off to eliminate parasitic absorption.

The n-contact was formed by 15 nm of InGe, followed by 150 nm of Au, which was annealed at 360°C. The *p*-contact was formed in a Au/Zn/Au configuration, with thicknesses of 5/20/150 nm respectively, which was followed by an anneal. The mask for the top contact grid can be seen in Fig. 7b. It has an opening of 3.25 mm in diameter, with 10 µm metal stripes spaced every 100 µm to ensure current collection across the device. Additionally, the solar cells were isolated from each other using a mesa etch step.

A total of 8 samples were produced, each having 9 individual solar cells. The J-V curve for the best performing solar cell can be seen in Fig. 9a. The best performing GaAsSbN solar cell achieved an efficiency 4.56%, V_{oc} of 0.5 V and J_{sc} of 20.82 $mAcm^{-2}$ and a fill factor 43.8 The general characteristic of the J-V indicates low shunt resistance values, perhaps as a consequence of lower than expected material quality. A typical EQE for the solar cells is shown in Fig. 9b. The results show the solar cell tuning into the 900 –1000 nm region. The CV measurement was also undertaken for the solar cell. The CV measurement indicated that the GaAsSbN layer was substantially more highly doped than the expected 10^{15} cm^{-3}, rather it was in the region of 10^{17} cm^{-3}. The consequence of this would mean that the field could not extend throughout the *p-in* structure sufficiently, and hence negatively impacted carrier collection, which resulted in the lower than expected solar cell performance.

a)

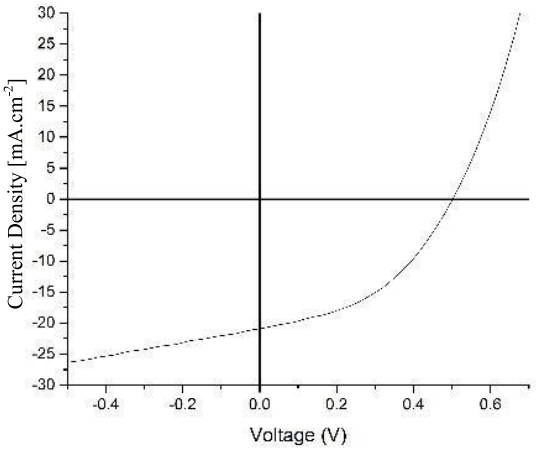

b)

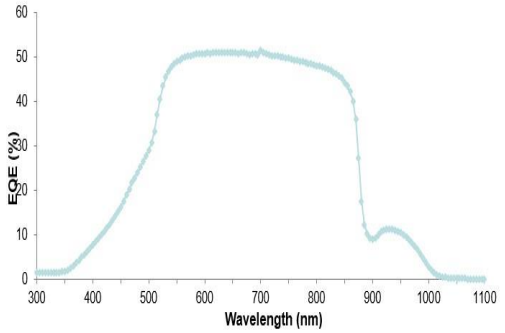

Fig. 8. a) J-V Curve b) EQE for GaAsSbN based solar cell

IV. SUMMARY

In conclusion, quaternary dilute nitride GaAsSbN layers were successfully grown using LPE without phase separation. The material was fully characterised in order to evaluate their electrical, structural and optical properties. A range of solar cells were produced and tested. A champion cell of 4.56% efficiency (V_{oc} of 0.5 V, J_{sc} of 20.82 mAcm^{-2}) was achieved, which is similar in performance to solar cells employing GaAsSbN fabricated using MOVPE and MBE. Analysis by CV measurements indicated that the doping profile in the GaAsSbN was significantly than expected, which has caused reduced performance.

ACKNOWLEDGMENT

The authors would like to thank Prof. Paul Warren, Dr Mark Farnworth from NSG Group and Prof. Tim Veal from the Stephenson Institute for Renewable Energy, University of Liverpool in supporting this work.

REFERENCES

[1] F. Dimroth *et al.*, "Four-Junction Wafer-Bonded Concentrator," *IEEE Journal of Photovoltaics*, vol. 6, no. 1, pp. 343-349, Jan. 2016.

[2] S. Kurtz and J. Geisz, "Multijunction solar cells for conversion of concentrated sunlight to electricity," *Optics Express*, vol. 18, no. S1, pp. 73–78, April 2010.

[3] A. Marti and G. L. Arafijo, "Limiting efficiencies for PV energy conversion in multigap systems," *Sol. Energy Mater. Sol. Cells*, vol. 43, pp. 203–222, 1996.

[4] S. R. Kurtz, D. Myers, and J. M. Olson, "Projected performance of threeand four-junction devices using GaAs and GaInP," in *26th IEEE Photovoltaics Specialists Conference*, 1997.

[5] W. Shan, W. Walukiewicz, and J. W. Ager III et al. "Band anticrossing in GaInNAs Alloys," *Phys. Rev. Lett.*, vol. 82, no. 6, pp. 1221–1224, 1999.

[6] D. J. Friedman and S. R. Kurtz, "Breakeven criteria for the GaInNAs junction in GaInP/GaAs/GaInNAs/Ge four-junction solar cells," *Prog. Photovoltaics Res. Appl.*, vol. 10, pp. 331–344, May 2002.

[7] J. F. Geisz, D. J. Friedman, J. M. Olson, S. R. Kurtz, and B. M. Keyes, "Photocurrent of 1 eV GaInNAs lattice-matched to GaAs," *J. Cryst. Growth*, vol. 195, pp. 401–408, 1998.

[8] D. J. Friedman, J. F. Geisz, A. G. Norman, M. W. Wanlass, and S. R. Kurtz, "0.7-eV GaInAs junction for a GaInP/GaAs/GaInAs(1eV)/GaInAs(0.7eV) four junction solar cell," *2006 IEEE 4th World Conf. Photovolt. Energy Conf.*, vol. 1, pp. 598–602, 2006.

[9] C. J. Hunter *et al.*, "Absorption characteristics of $GaAs_{1-x}Bi_x$/GaAs diodes in the near-IR," *IEEE Photonics Technol. Lett.*, vol. 24, pp. 2191–2194, 2012.

[10] G. Le Roux and J. C. Harmand, "GaAsSbN: a new low-bandgap material for GaAs substrates," *Electron. Lett.*, vol. 35, no. 15, pp. 861–863, 1999.

[11] K. H. Tan *et al.*, "Molecular beam epitaxy grown GaNAsSb 1 eV photovoltaic cell," *J. Cryst. Growth*, vol. 335, no. 2011, pp. 66–69, 2015.

[12] V. Sabnis, H. Yuen, M. Wiemer, "High-efficiency multijunction solar cells employing dilute nitrides," *AIP Conference Proceedings*, vol. 14, pp. 14–19.

[13] X. Yang, M. J. Jurkovic, J. B. Heroux, W. I. Wang, "Molecular beam epitaxial growth of InGaAsN:Sb/GaAs quantum wells for longwavelength semiconductor lasers," *Appl. Phys. Lett.*, vol. 178, May 1999, pp. 10–13, 2001.

[14] N. Ahsan, N. Miyashita, M. M. Islam, K. M. Yu, and W. Walukiewicz, "Effect of Sb on GaNAs intermediate band solar cells," *IEEE J. Photovoltaics*, vol. 3, no. 2, pp. 730–736, 2013.

[15] B. Kunert, W. Stolz, C. Baur, F. Dimroth, and A. W. Bett, "Optimization of annealing conditions of (GaIn)(NAs) for solar cell applications," vol. 310, pp. 2222–2228, 2008.

[16] T. W. Kim *et al.*, "Properties of 'bulk' GaAsSbN / GaAs for multijunction solar cell application: Reduction of carbon background concentration," *J. Cryst. Growth*, vol. 393, pp. 70–74, 2014.

[17] M. Milanova *et al*., "Study of GaAsSb:N bulk layers grown by liquid phase epitaxy for solar cells applications", Mater. Res. Express 6 075521, 2019.

[18] M. Milanova, V. Donchev, B. Arnaudov, D. Alonso-Álvarez, P. Terziyska, "GaAsSbN-based p-i-n heterostructures for solar cell applications grown by liquid-phase epitaxy", J. Mat. Sci.:Materials in Electronics 31 (3), pp. 2073–2080, 2020.

[19] L.F. Bian et al., "Photoluminescence characteristics of GaAsSbN/GaAs epilayers lattice-matched to GaAs substrates", Solid State Communications, 132, pp. 707–711, 2004.